PART 1

Discrete-Continuum Coupling Method to Model Highly Dynamic Multi-Scale Problems

1

State of the Art: Concurrent Discrete-continuum Coupling

1.1. Introduction

Some of the most fascinating dynamic problems in all fields of science involve multiple spatial or temporal scales: processes that occur at a certain scale govern the behavior of the system across several (usually coarser) scales. Therefore, to accurately simulate such problems with minimum cost, it is often necessary to resort to multi-scale modeling. In particular, the concurrent discrete-continuum coupling approaches seem to be the best adapted to study these problems. On the one hand, these approaches are of concurrent type. Therefore, as seen previously, these are well adapted to study highly dependent multi-scale phenomena, which are frequently encountered in complex dynamic problems. On the other hand, both discrete and continuum methods (CMs) are involved in these approaches. This allows us to combine their complementary advantages and to avoid their drawbacks. The complex small-scale phenomena can easily be treated by application of the discrete method (DM) in the associated regions. Furthermore, the application of the CM in the remainder of the studied domain significantly reduces the computation time, and avoids prohibitively large computations. Consequently, simulation of real problems of material science and engineering can be performed. Due to their advantages, the concurrent discrete-continuum coupling approaches have become very fashionable in the last decade. This chapter aims to shed light on some important aspects related to these approaches. First, the major challenges that the designer faces in developing such approaches will be outlined. Then, the coupling techniques most commonly used to address these challenges will be reviewed. The one that

best meets the scope of the present work will be selected. Although this review is not all-inclusive, it gives a clear vision of the topic. It should be noted that the techniques presented can also be applied for coupling DMs concurrently (concurrent discrete–discrete coupling).

1.2. Coupling challenges

Coupling dissimilar methods in a concurrent manner for dynamic analysis faces two major challenges. The first challenge is due to the different mechanics underlying the DM and CM. The second challenge is related to the different analysis scales of the coupled methods. This section is devoted to explaining these two challenges in more detail.

1.2.1. *Dissimilar variables due to different mechanical bases*

One major difficulty in coupling DM and CM is that these methods are based on different mechanics. The DMs are based on discrete mechanics, in which the interaction between neighboring discrete elements is described by classical Newtonian mechanics. The variables associated with this class of methods are only defined in the element positions. In contrast, the CMs are based on continuum mechanics, in which the studied domain is assumed to be continuous and completely filling the space it occupies. The mechanical behavior of this domain is described by constitutive laws involving continuous field variables, instead of discrete element variables as in the DMs. Therefore, a special treatment is required at the interface between the coupled methods to ensure correct communication between the coupled methods.

1.2.2. *Wave reflections due to different analysis scales*

Another major difficulty encountered in application of the concurrent discrete-continuum coupling approaches in dynamics is that, due to the different analysis scales, spurious wave reflections can occur at the interface between the coupled models. This difficulty is almost always encountered, since there is no benefit in coupling models having similar analysis scales. To simply illustrate the problem of spurious wave reflections, the behavior of waves in the discrete and continuum domains will be explored using simple one-dimensional (1D) models. A chain of particles connected with equivalent springs is used for the discrete model, and its corresponding continuum counterpart is used for the continuum model (Figure 1.1).

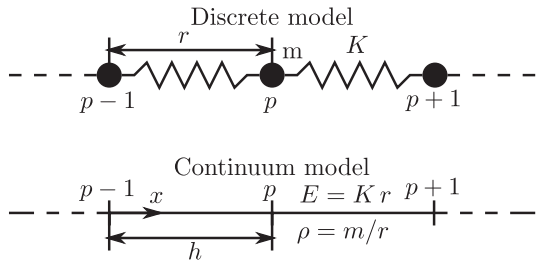

Figure 1.1. *1D models to investigate spurious wave reflections*

In the discrete model, the equation of motion of a particle p, in the absence of body forces, can be derived by application of the fundamental principle of dynamics (FPD):

$$m\,\ddot{d}^p = K\,(d^{p-1} - d^p) + K\,(d^{p+1} - d^p) = K\,(d^{p+1} + d^{p-1} - 2\,d^p) \qquad [1.1]$$

where K is the stiffness of the springs, and m and d^p are, respectively, the mass and displacement of the particle p. Equation [1.1] can be solved by assuming a wavelike solution which is only defined in the particle positions:

$$d^p = D\,e^{i\,(k\,p\,r - \omega\,t)} \qquad [1.2]$$

where D is the amplitude of the oscillations, k is the 1D wave vector (its amplitude gives the wavenumber $\kappa = |k| = \frac{2\pi}{\lambda}$), λ is the wave length, r is the interparticle distance ($x = p\,r$ is the position of the particle p along the chain) and ω is the angular frequency. Substituting [1.2] into [1.1] leads after simplification to:

$$\omega_D^2 = \frac{4\,K}{m} sin^2\left(\frac{k\,r}{2}\right) \qquad [1.3]$$

which is known as the dispersion relation. It characterizes the dependence of the wave frequency on the wavenumber $\kappa = |k|$. It can be shown from [1.3] that $\omega_D(k) = \omega_D(k + \frac{2\,j\,\pi}{r})$ for any $j \in \mathbb{Z}$. Therefore, only the case of $k \in [-\frac{\pi}{r}, \frac{\pi}{r}]$ will be considered hereafter. Moreover, for symmetry reasons, it is sufficient to restrict to $k = \kappa > 0$.

In the continuum model, the 1D equation of motion, in the absence of body forces, can be written as:

$$\rho\,\ddot{u} = \frac{\partial \sigma}{\partial x} \qquad [1.4]$$

where ρ is the density, and σ is the longitudinal Cauchy stress in x direction (Figure 1.1). Under the assumption of small deformations, equation [1.4] can be rewritten as:

$$\rho\,\ddot{u} = E\,\frac{\partial^2 u}{\partial x^2} \qquad [1.5]$$

where E is the Young's modulus. Assuming a harmonic wave propagating along the x direction ($u = U\,e^{i\,(k\,x-\omega\,t)}$), it is easy to find the continuum dispersion relation:

$$\omega_C^2 = \frac{E}{\rho}\,k^2 \qquad [1.6]$$

To ensure equivalence between the discrete and continuum models, E and ρ must verify, respectively, the following conditions (the cross-sectional area S is assumed to be equal to the unit, for simplicity):

$$E = K\,r \quad \text{and} \quad \rho = \frac{m}{r} \qquad [1.7]$$

Using these conditions [1.7], the continuum dispersion relation can be reformulated as follows:

$$\omega_C^2 = \frac{K\,r^2}{m}\,k^2 \qquad [1.8]$$

After obtaining the discrete and continuum dispersion relations ([1.3] and [1.8], respectively), the influence of the spatial and temporal discretization on these parameters will be examined. This allows us to better understand the wave reflection mechanisms encountered when coupling models of different scales.

1.2.2.1. *Influence of the spatial discretization on the dispersion relation*

In this section, the influence of the spatial discretization of the continuum model on the dispersion relation will be examined. To do this, the continuum domain is discretized into uniform segments of length h. Using linear interpolation functions, the discretized equation of motion of a node p can then be expressed as:

$$\rho\, h\, \ddot{u}^p = \frac{E}{h}\left(u^{p-1} - u^p\right) + \frac{E}{h}\left(u^{p+1} - u^p\right) = \frac{E}{h}\left(u^{p+1} + u^{p-1} - 2\,u^p\right) \quad [1.9]$$

where u^p designates the nodal displacement of the node p. By analogy with the discrete model and using [1.7], the dispersion relation of the discretized form of the continuum model can be obtained:

$$\tilde{\omega}_C^2 = \frac{4\,K\,r^2}{m\,h^2} sin^2\left(\frac{k\,h}{2}\right) \quad [1.10]$$

Using [1.3] and [1.10], the cutoff frequencies of the discrete and discretized continuum models can be obtained:

$$f_D^c = \frac{\omega_D^{max}}{2\pi} = \frac{1}{\pi}\sqrt{\frac{K}{m}} \quad [1.11]$$

$$\tilde{f}_C^c = \frac{\tilde{\omega}_C^{max}}{2\pi} = \frac{1}{\pi}\sqrt{\frac{K}{m}}\,\frac{r}{h} \quad [1.12]$$

The cutoff frequency of the discretized continuum model depends on h. In the case of coarse discretization ($h \gg r$), the associated cutoff frequency ($\tilde{f}_C^c$) becomes smaller than that of the discrete one (f_D^c). As a result, if these models are coupled, the high-frequency waves (HFWs) ($f > \tilde{f}_C^c$) coming from the discrete model are not supported by the continuum model, and will be spuriously reflected at the interface (Figure 1.2). This phenomenon has already been addressed using the finite element model with different element sizes [CEL 83].

Taking into account the assumption that $k = \kappa > 0$, the phase and group velocities in both the discrete model and discretized continuum model can be obtained from [1.3] and [1.10] as follows:

$$v_D^{ph} = \frac{\omega_D}{k} = \frac{2}{\kappa}\sqrt{\frac{C}{m}} sin\left(\frac{\kappa\,r}{2}\right) \quad \text{and} \quad v_D^{gr} = \frac{\partial \omega_D}{\partial k} = r\sqrt{\frac{C}{m}} cos\left(\frac{\kappa\,r}{2}\right) \quad [1.13]$$

$$\tilde{v}_C^{ph} = \frac{\omega_C}{k} = \frac{2}{\kappa}\frac{r}{h}\sqrt{\frac{C}{m}}\,sin\left(\frac{\kappa\, h}{2}\right) \quad \text{and}$$

$$\tilde{v}_C^{gr} = \frac{\partial \omega_C}{\partial k} = r\sqrt{\frac{C}{m}}cos\left(\frac{\kappa\, h}{2}\right) \qquad [1.14]$$

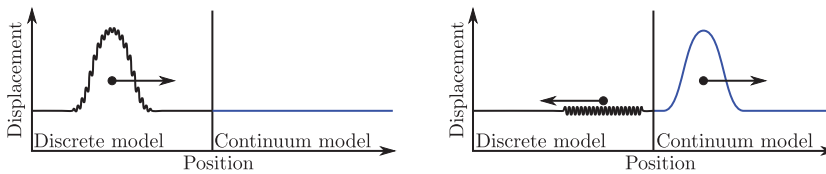

Figure 1.2. *Reflection of high-frequency waves at the interface between the discrete and continuum models*

The use of different discretization characteristic lengths in the discrete and continuum models (r and h) leads to different wave velocities. Moreover, for a fixed κ, the wave velocities in the discretized continuum model decrease as h increases. This explains another mechanism of wave reflections, for which a portion of the main propagating wave is reflected at the interface (not only the HFWs). Figure 1.3 presents examples of a wave traveling between two models having different wave propagation velocities, due to different spatial discretizations.

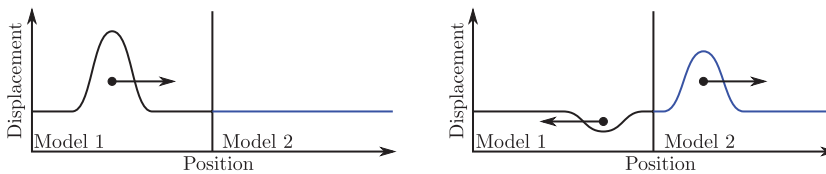

a) Wave traveling from a faster wave velocity model to a slower wave velocity model

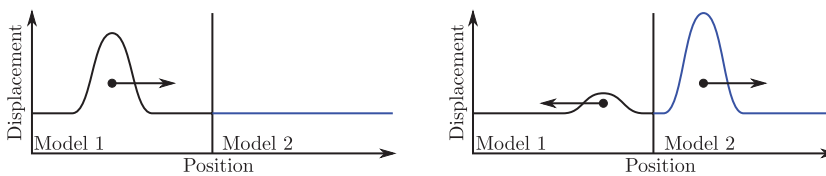

b) Wave traveling from a slower wave velocity model to a faster wave velocity model

Figure 1.3. *Wave traveling between two models having different wave propagation velocities*

1.2.2.2. *Influence of the temporal discretization on the dispersion relation*

As seen before, the use of different discretization characteristic lengths in the discrete and continuum models leads to different dispersion relations, and then to different phase and group velocities. Hereafter, the influence of the temporal discretization on the dispersion relations will be examined. For a given time step Δt, the second derivative of a field variable f with respect to time can be approximated as:

$$\ddot{f} \approx \frac{f_{t+\Delta t} - 2\, f_t + f_{t-\Delta t}}{(\Delta t)^2} \qquad [1.15]$$

Applying [1.15] to the particle and node accelerations ($\ddot{d}^p$ and $\ddot{u}^p$, respectively) and using the equivalence conditions [1.7], equations [1.1] and [1.9] can be approximated as:

$$\frac{m}{\Delta t_D^2}\,(d_{n+1}^p + d_{n-1}^p - 2\, d_n^p) = K\,(d_n^{p+1} + d_n^{p-1} - 2\, d_n^p) \qquad [1.16]$$

$$\frac{m}{\Delta t_C^2}\,(u_{n+1}^p + u_{n-1}^p - 2\, u_n^p) = K\,\frac{r^2}{h^2}\,(u_n^{p+1} + u_n^{p-1} - 2\, u_n^p) \qquad [1.17]$$

where Δt_D and Δt_C are, respectively, the discrete and the continuum time step, and d_n^p and u_n^p are, respectively, the displacement of a particle p and the displacement of a node p at the $n-th$ time step. By analogy with the derivation of the dispersion relations ([1.3] and [1.10]), the following equations can be obtained:

$$sin^2\left(\frac{\omega_D\,\Delta t_D}{2}\right) = \frac{K}{m}\,\Delta t_D^2\, sin^2\left(\frac{k\, r}{2}\right) \qquad [1.18]$$

$$sin^2\left(\frac{\tilde{\omega}_C\,\Delta t_C}{2}\right) = \frac{K}{m}\,\frac{r^2}{h^2}\,\Delta t_C^2\, sin^2\left(\frac{k\, h}{2}\right) \qquad [1.19]$$

Equations [1.18] and [1.19] are obtained using the general form of a harmonic solution which is expressed as $d_n^p = D\, e^{i\,(k\,p\,r - \omega\, n\, \Delta t_D)}$ for a particle p at the $n-th$ time step and $u_n^p = U\, e^{i\,(k\,p\,h - \omega\, n\, \Delta t_C)}$ for a node p at this time step. Using $k = \kappa > 0$, equations [1.18] and [1.19] can be rewritten as:

$$sin\left(\frac{\omega_D\,\Delta t_D}{2}\right) = \sqrt{\frac{K}{m}}\,\Delta t_D\, sin\left(\frac{\kappa\, r}{2}\right) \qquad [1.20]$$

$$sin\left(\frac{\tilde{\omega}_C\,\Delta t_C}{2}\right) = \sqrt{\frac{K}{m}}\,\frac{r}{h}\,\Delta t_C\,sin\left(\frac{\kappa\,h}{2}\right) \qquad [1.21]$$

With the help of the first-order and third-order Taylor expansions, an approximation of ω_D and $\tilde{\omega}_C$ can be obtained from [1.20] and [1.21] as follows:

$$\omega_D = \sqrt{\frac{K}{m}}\,k\,r\,\left[1 + \frac{k^2\,r^2}{24}\,\left(\frac{K}{m}\,\Delta t_D^2 - 1\right)\right] \qquad [1.22]$$

$$\tilde{\omega}_C = \sqrt{\frac{K}{m}}\,k\,r\,\left[1 + \frac{k^2\,h^2}{24}\,\left(\frac{K}{m}\,\frac{r^2}{h^2}\Delta t_C^2 - 1\right)\right] \qquad [1.23]$$

It can be concluded from the last two equations that, for different discretization characteristic lengths (r and h) and for a given discrete time step Δt_D, it is possible to choose a suitable Δt_C such that the dispersion relations of both models are equivalent:

$$\Delta t_C = \sqrt{\Delta t_D^2 + \frac{m}{K}\,\frac{h^2 - r^2}{r^2}} \qquad [1.24]$$

Therefore, the inaccurate continuum dispersion relation caused by large discretization characteristic length h can theoretically be corrected by choosing a larger continuum time step Δt_C. However, this solution is not always applicable in practice. For example, in the case of a "*dynamic explicit*" simulation, Δt_C must satisfy the Courant–Friedrichs–Lewy (CFL) stability criterion to ensure convergence of numerical approximation [1.25].

$$\Delta t_C \leq \frac{2\,\pi}{\tilde{\omega}_C^{max}} \qquad [1.25]$$

1.3. Coupling techniques

To correctly bridge DM and CM in a concurrent manner for dynamic analysis, the coupling challenges detailed in the previous section should be properly addressed. To this end, several techniques have been proposed in the literature [ABR 98, BRO 99, SMI 99, LU 05, XU 09, JEB 14, CUR 03]. A common feature of these techniques is that the problem domain is often partitioned into several subdomains characterized by different scales and physics. The question that arises here is how to ensure a smooth coupling between these subdomains. The next section tries to answer this question by reviewing the most used techniques.

1.3.1. *Edge-to-edge coupling methods*

A common technique for coupling discrete and continuum models is the edge-to-edge approach. This technique is also widely used in the finite element community for parallel implementation of the finite element method (FEM) method [ZHU 01]. As shown in Figure 1.4, two types of discrete elements are used in this technique. Aside from the real elements, virtual elements are defined to model the angle-bending of the bonds (virtual) between the discrete model and continuum model. The virtual particles (discrete elements) are connected on one side to the discrete model by virtual bonds, and on the other side are attached to the continuum model and move with it. The motion of these particles can be determined by interpolation of the continuum node motion. The most simple variation of this technique is that in which the particles and continuum nodes on the interface are coincident and constrained to move together. This variation is known in the literature as the direct coupling approach. In the general case, the coincidence of particles and nodes on the interface is not necessary. In this case, additional handling is required to ensure correct communication between the coupled models. This last point will be discussed below in more detail.

A domain Ω_G is considered with boundary $\partial\Omega = \partial\Omega^u \cup \partial\Omega^t$ ($\partial\Omega^u \cap \partial\Omega^t = \phi$), such that essential (displacement) and natural (traction) boundary conditions are, respectively, prescribed on $\partial\Omega^u$ and $\partial\Omega^t$. This domain is divided into two adjacent subdomains Ω_D and Ω_C. These subdomains are, respectively, modeled using the discrete approach and continuum approach (Figure 1.4). An isotropic linear elastic behavior and small deformations are assumed for simplicity. In the present development, an energetic (Hamiltonian) approach will be used to derive the governing equations of the coupling system.

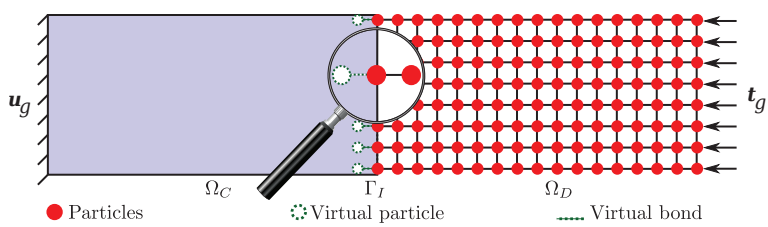

Figure 1.4. *Edge-to-edge coupling*

The total energy in the discrete subdomain Ω_D, which is assumed to be isolated at this stage, is known as the Hamiltonian and is given by:

$$\begin{aligned} H_D &= E_D^{kinetic} + E_D^{int} - W_D^{ext} \\ &= \sum_{i=1}^{n_D} \frac{1}{2\,m_i} \left(\boldsymbol{p}_D^i\right)^2 - \sum_{i=1}^{n_D} \boldsymbol{f}_i^{int}\,\boldsymbol{d}_i + E_D^{virtual} - \sum_{i=1}^{n_D} \boldsymbol{f}_i^{ext}\,\boldsymbol{d}_i \end{aligned} \qquad [1.26]$$

where $E_D^{kinetic}$ is the kinetic energy, E_D^{int} is the internal energy, W_D^{ext} is the external work, n_D is the total number of particles, m_i and $\boldsymbol{p}_D^i = m_i\,\dot{\boldsymbol{d}}_i$ are the mass and momentum of the particle i, $\boldsymbol{d}_i$ and $\dot{\boldsymbol{d}}_i$ are, respectively, the displacement and velocity of the particle i, $\boldsymbol{f}_i^{int}$ is the total internal force exerted on the particle i by its neighbors, $\boldsymbol{f}_i^{ext}$ is the total external force acting on the particle i and $E_D^{virtual}$ is the bending energy of the virtual bonds. It should be noted that the stretching energy of the virtual bonds is automatically included in the continuum internal energy, since the virtual particles move with the continuum material. At this stage, $\boldsymbol{f}_i^{ext}$ does not include the coupling force which will be introduced later.

Under the assumption of small deformations, the total energy in the continuum subdomain Ω_C, which is supposed to be isolated at this stage, can be written as:

$$\begin{aligned} H_C &= E_C^{kinetic} + E_C^{int} - W_C^{ext} \\ &= \int_{\Omega_C} \frac{1}{2}\,\rho\,\dot{\boldsymbol{u}}^2\,d\Omega + \tfrac{1}{2}\int_{\Omega_C} \boldsymbol{\sigma} : \boldsymbol{\varepsilon}\,d\Omega - \textstyle\int_{\Omega_C} \rho\,\boldsymbol{b}\,\boldsymbol{u}\,d\Omega - \int_{\partial\Omega_C^t} \boldsymbol{t}_g\,\boldsymbol{u}\,d\Gamma \end{aligned} \qquad [1.27]$$

where ρ is the density and $\dot{\boldsymbol{u}}$ is the velocity field, $\boldsymbol{\sigma}$ and $\boldsymbol{\varepsilon}$ are, respectively, the Cauchy stress tensor and strain tensor, $\boldsymbol{b}$ is the body force per unit mass and $\boldsymbol{t}_g$ is the prescribed traction vector on $\partial\Omega_C^t$.

In the above development, the discrete and continuum energies are derived without taking into account the coupling conditions. In the following, it will be shown how these models are coupled. Generally, the compatibility at the interface between the coupled models can be enforced using either velocity constraints or displacement constraints. However, in the case of highly dynamic problems, where dynamic effects become significant, it would be preferable to use velocity constraints to ensure a correct kinetic energy transfer between the coupled models. For the sake of consistency with the energetic (Hamiltonian) approach followed here to develop the edge-to-edge coupling method, displacement constraints will be used in the rest of this

derivation. These constraints can be applied in different ways, as shown in [1.28] and [1.29].

$$g_i^{weak} = \|\boldsymbol{u}(\boldsymbol{x}_i) - \boldsymbol{d}_i\|^2 = 0, \quad i \in [1,\, n_{DI}] \qquad [1.28]$$

$$g_i^{strong} = \boldsymbol{u}(\boldsymbol{x}_i) - \boldsymbol{d}_i = \boldsymbol{0}, \quad i \in [1,\, n_{DI}] \qquad [1.29]$$

$\boldsymbol{u}$ is the continuum displacement field, $\boldsymbol{d}_i$ is the displacement of a particle i located on the interface at $\boldsymbol{x}_i$ coordinates and n_{DI} is the number of particles on the interface. In [1.28], a single constraint is applied per particle belonging to the interface. This results in a system of equations with a reduced number of degrees of freedom. However, using this type of constraint, displacement compatibility is only satisfied approximately. This can lead to unacceptable large errors. In contrast, three constraints (one for each component) per particle are applied in [1.29]. This allows the coupled models to better communicate. Although it can lead to a large system of equations, [1.29] is generally recommended and is retained here to enforce compatibility between the discrete and continuum approaches. In practice, these constraints can be introduced in the global system by using rigid models, such as the Lagrangian multipliers model (LM), elastic models such as the penalty model (PM) or combined models such as the augmented Lagrange multipliers model (ALM). In the rest of this derivation, the ALM is used, because it is more general and includes the two other models. The associated coupling energy, in a continuous form, is given by:

$$H_I^{ALM} = \int_{\Gamma_I} \boldsymbol{\lambda}\,(\boldsymbol{u} - \boldsymbol{d})\,d\Gamma + \frac{p}{2}\int_{\Gamma_I} (\boldsymbol{u} - \boldsymbol{d})^2\,d\Gamma \qquad [1.30]$$

where Γ_I is the interface between the two models, $\boldsymbol{\lambda}$ is the Lagrange multipliers field and p is the penalty parameter. The Lagrange multipliers field $\boldsymbol{\lambda}$ can be regarded as a generalized coupling force field. Since the displacements $\boldsymbol{d}_i$ in the discrete subdomain Ω_D are only defined in the particle positions, a continuous field $\boldsymbol{d}$ must be inferred from the particle displacements $\boldsymbol{d}_i$ at least on the interface to evaluate H_I^{ALM} [1.30]. This can be achieved using a kind of interpolation:

$$\boldsymbol{d}(\boldsymbol{x}_i) = \sum_{j=1}^{n_{DI}} \phi_D^j(\boldsymbol{x}_i)\,\boldsymbol{d}_j \qquad [1.31]$$

where ϕ_D^j is the interpolation function associated with the particle j. Taking into account [1.30], the total energy of the coupling system can be obtained:

$$H_G^{ALM} = H_D + H_C + H_I^{ALM} \qquad [1.32]$$

In [1.32], the Hamiltonian is given in a continuous form. To develop the corresponding discrete form $\tilde{H}_G^{ALM}$, the continuum displacement and the Lagrange multipliers fields ($\boldsymbol{u}$ and $\boldsymbol{\lambda}$, respectively) can be approximated, using, for example, the finite element interpolation in the corresponding domains, as follows:

$$\tilde{\boldsymbol{u}}(\boldsymbol{x}) = \sum_{i=1}^{n_C} \phi_C^i(\boldsymbol{x})\, \boldsymbol{u}_i \qquad [1.33]$$

$$\tilde{\boldsymbol{\lambda}}(\boldsymbol{x}) = \sum_{i=1}^{n_I} \phi_I^i(\boldsymbol{x})\, \boldsymbol{\lambda}_i \qquad [1.34]$$

where ϕ_C^i and ϕ_I^i are the shape functions constructed on, respectively, $\tilde{\Omega}_C$ and $\tilde{\Gamma}_I$ (the discretized forms of, respectively, Ω_C and Γ_I), n_C and n_I are, respectively, the total number of continuum nodes and the total number of Lagrange multipliers nodes. In the general case, the Lagrange multipliers nodes do not necessarily coincide with the discrete particles or the continuum nodes at the interface. Substituting [1.33] and [1.34] into [1.32] and using [1.31] on Γ_I, the discrete Hamiltonian $\tilde{H}_G^{ALM}$ can be obtained. Based on $\tilde{H}_G^{ALM}$, the discretized Hamiltonian equations of the coupling system can be derived:

$$\dot{\boldsymbol{p}}_D^i = -\frac{\partial \tilde{H}_G^{ALM}}{\partial \boldsymbol{d}_i}, \quad \text{and} \quad \dot{\boldsymbol{d}}_i = \frac{\partial \tilde{H}_G^{ALM}}{\partial \dot{\boldsymbol{p}}_D^i} \quad \text{for } i \in [1,\, n_D] \qquad [1.35]$$

$$\dot{\boldsymbol{p}}_C^i = -\frac{\partial \tilde{H}_G^{ALM}}{\partial \boldsymbol{u}_i} \quad \text{and} \quad \dot{\boldsymbol{u}}_i = \frac{\partial \tilde{H}_G^{ALM}}{\partial \dot{\boldsymbol{p}}_C^i} \quad \text{for } i \in [1,\, n_C] \qquad [1.36]$$

$$g_i = \frac{\partial \tilde{H}_G^{ALM}}{\partial \boldsymbol{\lambda}_i} = 0 \quad \text{for } i \in [1,\, n_I] \qquad [1.37]$$

Replacing $\dot{\boldsymbol{d}}_i$ and $\dot{\boldsymbol{u}}_i$ with their expressions in, respectively, $\dot{\boldsymbol{p}}_D^i$ and $\dot{\boldsymbol{p}}_C^i$, the global system of equations can be expressed, in matrix form, as:

$$\boldsymbol{m}\, \ddot{\boldsymbol{d}} = \boldsymbol{f}^{int} + \boldsymbol{f}^{ext} + \boldsymbol{f}^{\lambda} \qquad [1.38]$$

$$\boldsymbol{M}\ddot{\boldsymbol{u}} = \boldsymbol{F}^{int} + \boldsymbol{F}^{ext} - \boldsymbol{F}^{\lambda} \quad [1.39]$$

$$\boldsymbol{C}_I\boldsymbol{u} - \boldsymbol{c}_I\,\boldsymbol{d} = 0 \quad [1.40]$$

where $\boldsymbol{m}$ is the diagonal mass matrix of the particles, $\boldsymbol{f}^{int}$, $\boldsymbol{f}^{ext}$ and $\boldsymbol{f}^{\lambda}$ are the vectors of, respectively, the internal forces, external forces and coupling forces in the discrete model, $\boldsymbol{M}$ is the lumped mass matrix of the nodes, $\boldsymbol{F}^{int}$, $\boldsymbol{F}^{ext}$ and $\boldsymbol{F}^{\lambda}$ are the vectors of, respectively, the internal forces, external forces and coupling forces in the continuum model, $\boldsymbol{C}_I$ and $\boldsymbol{c}_I$ are the continuum and discrete coupling matrices. The matrix systems [1.47], [1.48] and [1.49] are in the form of time-dependent ordinary differential equations (ODEs). These equations can be solved numerically using a time integration scheme.

The edge-to-edge coupling methods are rather dedicated to quasi-static problems or problems with relatively low dynamic effects. Otherwise, fine discretization of the continuum subdomain, at the same level as the discrete subdomain, is required to deal with the spurious wave reflections at the interface. Moreover, in most of the cases, the use of fine continuum discretization is not sufficient to overcome the reflection problems. Mostly, the particles belonging to the interface must be coupled with dampers, which are generally difficult to adjust. These difficulties make the edge-to-edge coupling approaches useless for dynamic studies, since the reduction in the computation effort from a fully discrete element analysis is not significant.

1.3.2. *Bridging domain coupling methods*

In the following, the bridging (overlapping) domain (BD) technique for coupling continuum models with discrete models is described. Contrary to the edge-to-edge coupling technique, the present technique considers a BD (overlapping) between the coupled models. It should be noted that this technique is also called the Arlequin approach in the literature [BEN 98, BEN 01, BEN 05]. It consists of:

– decomposition of the global domain Ω_G into two subdomains Ω_D and Ω_C, modeled, respectively, by the discrete model and continuum model, with a bridging region Ω_B;

– weak coupling (based on weak formulation): the discrepancy between the mechanical states, e.g. displacement, deformation, strain, etc., in the bridging region must be controlled using some kind of fictive forces. To allow each model to express its own wealth, the discrepancy should preferably be controlled in a weak manner using averaging operators. This point consists of:

- definition of a gluing zone Ω_{GL} ($\Omega_{GL} \subseteq \Omega_B$), in which the coupling control will be performed. In the general case, this zone can be different from the bridging region ($\Omega_{GL} \subsetneq \Omega_B$). In the present development, Ω_{GL} is chosen the same that Ω_B. Hereafter, the term "bridging zone" will be used to designate both the bridging zone and gluing zone,

- definition of a mediator space $\mathcal{M}$ which is defined as the space of the field variables restricted to Ω_B that must be controlled in the bridging region. To ensure a correct dialogue between the coupled models, the control quantities must be carefully chosen. Generally, either displacements or velocities are controlled in Ω_B,

- definition of a projection operator Π which will be used to project the discrete and continuum field variables to be controlled onto the mediator space $\mathcal{M}$,

- definition of a junction model which will be used to ensure the compatibility of the controlled field variables in the bridging region. Besides the Lagrange, penalty and augmented Lagrange multipliers models, which were introduced earlier, another junction model has been proposed in the literature [BAU 08, BEN 01, BEN 98, BEN 05, BEN 08]:

$$< \boldsymbol{\lambda}, \boldsymbol{f}_C - \boldsymbol{f}_D > = \int_{\Omega_B} \eta_1 \, \boldsymbol{\lambda} \cdot (\Pi \boldsymbol{f}_C - \Pi \boldsymbol{f}_D) + \eta_2 \, l^2 \boldsymbol{\varepsilon}(\boldsymbol{\lambda}) : \boldsymbol{\varepsilon}(\Pi \boldsymbol{f}_C - \Pi \boldsymbol{f}_D) \, d\Omega \qquad [1.41]$$

where $(\Pi \boldsymbol{f}_C - \Pi \boldsymbol{f}_D)$ is the difference between the projected continuum and discrete control quantities on the mediator space $\mathcal{M}$, $\boldsymbol{\lambda}$ is the Lagrange multiplier field and l is a parameter which is named "*junction parameter*" in this book. This parameter which has the dimension of a length is added to ensure the homogeneity of the integral terms in [1.41]. η_1 and η_2 are non-negative weight parameters. These parameters can be chosen so as to scale the two integral terms in [1.41]. $(\eta_1, \eta_2) = (1, 0)$ refers to $\mathcal{L}^2(\Omega_B)$ inner (scalar) product which is the same that the Lagrange multiplier model, $(\eta_1, \eta_2) = (1, 1)$ refers to $\mathcal{H}^1(\Omega_B)$ inner (scalar) product and $(\eta_1, \eta_2) = (0, 1)$ refers to $\mathcal{H}^1(\Omega_B)$ semi-inner product;

– partition of energy between the discrete and continuum models in the bridging zone. The two models coexist in Ω_B. Therefore, the discrete and continuum energies in this region must be weighted using a kind of unity partition functions (to avoid counting twice the associated energy). Different weight functions can be used for the kinetic energy, internal energy and

external work in Ω_B. These functions must verify:

$$f_C : \Omega_G \mapsto [0,1] \qquad x \mapsto \begin{cases} 1 & \text{in } \Omega_C \backslash \Omega_B \\ [0,1] & \text{in } \Omega_B \\ 0 & \text{in } \Omega_D \backslash \Omega_B \end{cases} \qquad [1.42]$$

in the continuum subdomain, and $f_D = \bar{f}_C = 1 - f_C$ in the discrete subdomain. Figure 1.5 presents examples of weight functions.

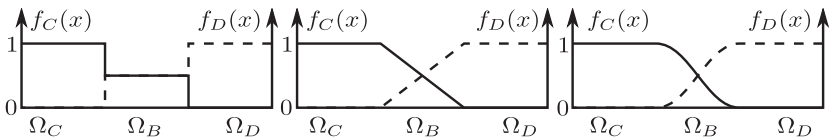

(a) Discontinous (b) Linear continuous (c) Continuous differential

Figure 1.5. *Examples of weight functions*

These different ingredients will be detailed hereafter. As for the edge-to-edge technique, a domain Ω_G is considered with boundary $\partial\Omega = \partial\Omega^u \cup \partial\Omega^t$ ($\partial\Omega^u \cap \partial\Omega^t = \phi$), such that essential (displacement) and natural (traction) boundary conditions are, respectively, prescribed on $\partial\Omega^u$ and $\partial\Omega^t$. This domain is divided into two subdomains Ω_D, treated by the discrete model, and Ω_C, treated by the continuum model, with a bridging region Ω_B (Figure 1.6). An isotropic linear elastic behavior and small deformations are assumed for simplicity.

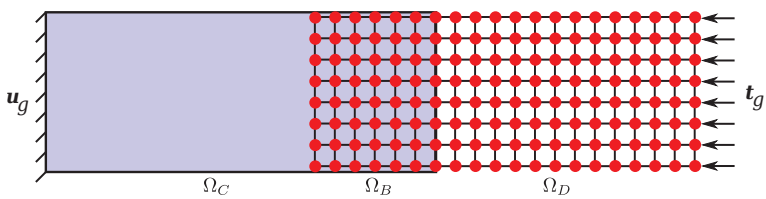

Figure 1.6. *Bridging domain coupling*

To weight the energies in the continuum subdomain, three weight functions are assumed in this development: α for the internal energy, β for the kinetic energy and γ for the external work. In a complementary manner, the energies

in the discrete subdomain are weighted using $\bar{\alpha}$, $\bar{\beta}$ and $\bar{\gamma}$, for, respectively, the internal energy, kinetic energy and external work. Using these functions, the weighted discrete and continuum Hamiltonians can, respectively, be written as:

$$\begin{aligned} H_D^w &= E_D^{kinetic,\,w} + E_D^{int,\,w} - W_D^{ext,\,w} \\ &= \sum_{i=1}^{n_D} \frac{1}{2\,m_i}\,\bar{\beta}_i\,\left(\boldsymbol{p}_D^i\right)^2 - \sum_{i=1}^{n_D} \bar{\alpha}_i\,\boldsymbol{f}_i^{int}\,\boldsymbol{d}_i - \sum_{i=1}^{n_D} \bar{\gamma}_i\,\boldsymbol{f}_i^{ext}\,\boldsymbol{d}_i \end{aligned} \quad [1.43]$$

$$\begin{aligned} H_C^w &= E_C^{kinetic,\,w} + E_C^{int,\,w} - W_C^{ext,\,w} \\ &= \int_{\Omega_C} \frac{1}{2}\,\beta\,\rho\,\dot{\boldsymbol{u}}^2\,d\Omega + \frac{1}{2}\int_{\Omega_C} \alpha\,\boldsymbol{\sigma} : \boldsymbol{\varepsilon}\,d\Omega \\ &\quad - \int_{\Omega_C} \gamma\,\rho\,\boldsymbol{b}\,\boldsymbol{u}\,d\Omega - \int_{\partial\Omega_C^t} \gamma\,\boldsymbol{t}_g\,\boldsymbol{u}\,d\Gamma \end{aligned} \quad [1.44]$$

To enforce compatibility between the coupled models in the bridging zone Ω_B, the $\mathcal{H}^1(\Omega_B)$ junction model ([1.41], with $(\eta_1,\,\eta_2) = (1,\,1)$) is used. The associated coupling energy can be written as:

$$H_B^{H1} = \int_{\Omega_B} \boldsymbol{\lambda} \cdot (\Pi\boldsymbol{u} - \Pi\boldsymbol{d}) + l^2\boldsymbol{\varepsilon}(\boldsymbol{\lambda}) : \boldsymbol{\varepsilon}(\Pi\boldsymbol{u} - \Pi\boldsymbol{d})\,d\Omega \quad [1.45]$$

As explained before, to evaluate H_B^{H1}, a continuous displacement field $\boldsymbol{d}$ must be approximated from the particle displacements $\boldsymbol{d}_i$ in the bridging zone, using a kind of interpolation [1.31]. The global Hamiltonian of the coupling system can be obtained by summing [1.43], [1.44] and [1.45]:

$$H_G^{H1} = H_D^w + H_C^w + H_B^{H1} \quad [1.46]$$

To obtain the corresponding discrete form $\tilde{H}_G^{H1}$, the continuum displacement field $\boldsymbol{u}$ and the Lagrange multipliers field $\boldsymbol{\lambda}$ are approximated as given by [1.33] and [1.34]. Using $\tilde{H}_G^{H1}$, the global system of equations can be derived:

$$\boldsymbol{m}_\beta\,\ddot{\boldsymbol{d}} = \boldsymbol{f}_\alpha^{int} + \boldsymbol{f}_\gamma^{ext} + \boldsymbol{f}^\lambda \quad [1.47]$$

$$\boldsymbol{M}_\beta\,\ddot{\boldsymbol{u}} = \boldsymbol{F}_\alpha^{int} + \boldsymbol{F}_\gamma^{ext} - \boldsymbol{F}^\lambda \quad [1.48]$$

$$\boldsymbol{C}_B\,\boldsymbol{u} - \boldsymbol{c}_B\,\boldsymbol{d} = 0 \quad [1.49]$$

where $\boldsymbol{m}_\beta$ is the weighted diagonal mass matrix of the particles, $\boldsymbol{f}_\alpha^{int}$, $\boldsymbol{f}_\gamma^{ext}$ and $\boldsymbol{f}^\lambda$ are, respectively, the weighted vector of internal forces, weighted vector of external forces and vector of coupling forces in the discrete model, $\boldsymbol{M}_\beta$ is the weighted continuum lumped mass matrix, $\boldsymbol{F}_\alpha^{int}$, $\boldsymbol{F}_\gamma^{ext}$ and $\boldsymbol{F}^\lambda$ are, respectively, the weighted vector of internal forces, weighted vector of the external forces and vector of coupling forces in the continuum model. $\boldsymbol{C}_B$ and $\boldsymbol{c}_B$ are the continuum and discrete coupling matrices. For $\boldsymbol{M}_\beta$ and $\boldsymbol{m}_\beta$ to be invertible, the weight functions β and $\bar{\beta}$ must be strictly positive in Ω_B and at the border $\partial\Omega_B$. Therefore, a small ε must be used instead of zero in the nodes assigned to $\partial\Omega_B$. The definition of the weight function β given by [1.42] is slightly modified as follows:

$$\begin{array}{rcl} \beta : \Omega_G & \rightarrow & [0,1] \\ x & \rightarrow & \begin{cases} 1 & \text{in } \Omega_C \backslash \Omega_B \\ [\varepsilon, 1-\varepsilon] & \text{in } \Omega_{C|\Omega_B} \\ 0 & \text{in } \Omega_D \backslash \Omega_B \end{cases} \end{array} \qquad [1.50]$$

The global system of equations consisting of [1.47], [1.48] and [1.49] can finally be solved using a temporal integration scheme.

In the BD coupling methods, the fine-scale solution (of the discrete model) is continuously projected onto the coarse-scale solution (of the continuum model) in the bridging zone. This can cancel the HFWs, and then avoids spurious wave reflections at the discrete/continuum interface, without any additional filtering or damping [BEN 05, JEB 13c]. However, this is conditional upon choosing correctly the coupling parameters, which is not a straightforward issue due to the large number of these parameters. Another interesting aspect of the BD coupling methods is that they can also be applied to obtain solution for nonlinear problems, in which devising an energy functional for the entire system is not possible, due to the presence of irreversible process, for example [FIS 07].

1.3.3. *Bridging-scale coupling methods*

The bridging-scale technique was recently proposed by Wagner and Liu [WAG 03] to couple molecular dynamics (MD) and FEM. The main concepts of this approach will be briefly reviewed hereafter. The readers can refer to [PAR 05a, PAR 05b, WAG 03] for more details. Two subdomains Ω_D and Ω_C modeled, respectively, by discrete and continuum models are considered. These will first be assumed to be completely superimposed in the global domain Ω_G, to better understand the features of the bridging-scale approach.

The key idea of such an approach is to decompose the total displacement field $\boldsymbol{u}$ in the particle positions into coarse and fine scales:

$$\boldsymbol{u}_{Tot}(\boldsymbol{x}_i) = \bar{\boldsymbol{u}}(\boldsymbol{x}_i) + \boldsymbol{u}'(\boldsymbol{x}_i) \quad [1.51]$$

where $\boldsymbol{x}_i$ represents the position of a particle i, $\bar{\boldsymbol{u}}$ and $\boldsymbol{u}'$ are, respectively, the coarse-scale and fine-scale displacements (Figure 1.7).

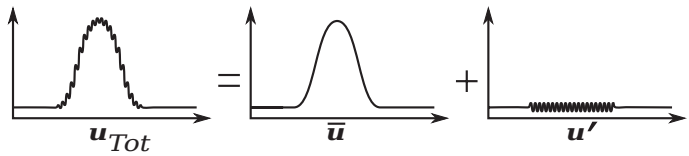

Figure 1.7. *Scale decomposition of total displacement in the particle positions*

After discretization of the continuum subdomain Ω_C, the coarse-scale displacement in the particle positions $\boldsymbol{x}_j$ is evaluated from the continuum nodal displacements as:

$$\bar{\boldsymbol{u}}(\boldsymbol{x}_j) = \sum_{i=1}^{n_C} \phi_C^i(\boldsymbol{x}_j)\, \boldsymbol{u}_i \quad [1.52]$$

where $\boldsymbol{u}_i$ and ϕ_C^i are the continuum nodal displacement and shape function associated with the node i, respectively. For the sake of clarity, matrix representation will be used for subsequent developments. In matrix form, equation [1.52] can be rewritten as:

$$\bar{\boldsymbol{u}} = \boldsymbol{N}\, \boldsymbol{u} \quad [1.53]$$

where $\bar{\boldsymbol{u}} = {}^t\{\bar{\boldsymbol{u}}(\boldsymbol{x}_1)\ \bar{\boldsymbol{u}}(\boldsymbol{x}_2)\ ...\ \bar{\boldsymbol{u}}(\boldsymbol{x}_{n_D})\}$ is the vector of coarse displacements in the particles positions, n_D is the total number of particles, $\boldsymbol{u} = {}^t\{\boldsymbol{u}_1\ \boldsymbol{u}_2\ ...\ \boldsymbol{u}_{n_C}\}$ is the vector of continuum nodal displacements, n_C is the total number of nodes and $\boldsymbol{N}$ is the interpolation matrix.

The fine-scale displacement is defined as the part of the total displacement that cannot be represented by the coarse scale. This quantity is computed from the vector $\boldsymbol{d}$ of the particle displacements, which include the

coarse-scale parts, by subtracting (from $\boldsymbol{d}$) the projection of the discrete solution onto the continuum solution.

$$\begin{aligned} \boldsymbol{u}' &= \boldsymbol{d} - \boldsymbol{P}\,\boldsymbol{d} \\ &= \boldsymbol{Q}\,\boldsymbol{d} \end{aligned} \qquad [1.54]$$

where $\boldsymbol{P}$ is the projection matrix and $\boldsymbol{Q} = \boldsymbol{I} - \boldsymbol{P}$ is the complementary projector [WAG 03]. The term $\boldsymbol{P}\,\boldsymbol{d}$, which is called "bridging scale (BS)", is the part of the particle displacement that must be subtracted from the total displacement to completely separate the scales (i.e. the coarse and fine scales are orthogonal or linearly independent of each other). The total displacement $\boldsymbol{u}$ can finally be written as the sum of the coarse and fine scales as:

$$\boldsymbol{u}_{Tot} = \boldsymbol{N}\,\boldsymbol{u} + \boldsymbol{Q}\,\boldsymbol{d} \qquad [1.55]$$

To derive the coupled discrete and continuum equations, it is most convenient to adopt the Lagrangian approach, in which the multi-scale Lagrangian is defined by:

$$\begin{aligned} L(\boldsymbol{u}_{Tot},\, \dot{\boldsymbol{u}}_{Tot}) &= E^{kinetic}(\dot{\boldsymbol{u}}_{Tot}) - E^{int}(\boldsymbol{u}_{Tot}) + W^{ext}(\boldsymbol{u}_{Tot}) \\ &= \tfrac{1}{2}\,{}^t\dot{\boldsymbol{u}}\,\boldsymbol{M}\,\dot{\boldsymbol{u}} + \tfrac{1}{2}\,{}^t\dot{\boldsymbol{d}}\,\boldsymbol{m}_f\,\dot{\boldsymbol{d}} - E^{int}(\boldsymbol{u}_{Tot}) + {}^t\,\boldsymbol{f}^{ext}\,\boldsymbol{u}_{Tot} \end{aligned} \qquad [1.56]$$

where $\boldsymbol{M}$ and $\boldsymbol{m}_f$ are, respectively, the coarse-scale and fine-scale diagonal mass matrices (defined in terms of the diagonal mass matrix $\boldsymbol{m}$ of the particles as: $\boldsymbol{M} = \boldsymbol{N}^t\,\boldsymbol{m}\,\boldsymbol{N}$ and $\boldsymbol{m}_f = \boldsymbol{Q}^t\,\boldsymbol{m}\,\boldsymbol{Q} = \boldsymbol{Q}^t\,\boldsymbol{m} = \boldsymbol{m}\,\boldsymbol{Q}$), and $\boldsymbol{f}^{ext}$ is the vector of external forces acting on the particles. An important feature of the Lagrangian [1.56] is the absence of quadratic terms in the kinetic energy, which are canceled due to the presence of the "BS". The coupled multi-scale equations of motion can be obtained from L as follows:

$$\frac{d}{dt}\left(\frac{\partial L}{\partial \dot{\boldsymbol{u}}}\right) - \frac{\partial L}{\partial \boldsymbol{u}} = 0 \quad \text{and} \quad \frac{d}{dt}\left(\frac{\partial L}{\partial \dot{\boldsymbol{d}}}\right) - \frac{\partial L}{\partial \boldsymbol{d}} = 0 \qquad [1.57]$$

Using [1.56], these equations can be rewritten after simplification as:

$$\boldsymbol{m}\ddot{\boldsymbol{d}} = \boldsymbol{f}^{int} + \boldsymbol{f}^{ext} \qquad [1.58]$$

$$\boldsymbol{M}\ddot{\boldsymbol{u}} = \boldsymbol{N}^t\left(\boldsymbol{f}^{int} + \boldsymbol{f}^{ext}\right) \qquad [1.59]$$

The first (fine scale) equation is the equation of motion in the discrete model, $\boldsymbol{m}$ is the diagonal mass matrix of the particles. The second (coarse

scale) equation is simply the equation of motion in the continuum model, where the mass matrix $\boldsymbol{M}$ is consistent. The coupling between these equations is ensured through the vector of the continuum internal forces $\boldsymbol{F}^{int} = \boldsymbol{N}^t \boldsymbol{f}^{int}$ which is a function of the vector of the discrete internal forces $\boldsymbol{f}^{int}$.

In the above development, Ω_D and Ω_C are assumed to be completely superimposed. In this case, the continuum equation of motion [1.59] is redundant, since it is only an approximation of the discrete one [1.58]. The total and discrete displacements ($\boldsymbol{u}_{Tot}$ and $\boldsymbol{d}$, respectively) satisfy the same equation of motion [1.58] and have the same initial conditions. Therefore, these quantities are identical during the entire simulation, and the continuum displacement $\boldsymbol{u}$ can simply be determined by [1.55] which implies: $\boldsymbol{N}\,\boldsymbol{u} = \boldsymbol{P}\,\boldsymbol{d}$.

Assuming that the fine-scale analysis is only required in a small region Ω_B, the particles outside this zone will now be removed. In other words, the unnecessary fine-scale degrees of freedom will be eliminated. By doing so, the discrete model is reduced to Ω_B, where the two models coexist, and the remaining estate is only modeled by the continuum model (Figure 1.8). The process of eliminating the unnecessary degrees of freedom results in a modified equation of motion in the discrete model, including an external force called impedance force. This force is a function of a damping matrix or equivalently its time derivative, known as the time history kernel [ADE 76, WAG 03]. The damping kernel was first derived analytically by Adelman and Doll [ADE 76] for a harmonic 1D lattice. However, their analytical approach is very costly and is intractable above 1D [PAR 05b]. To overcome this limitation, other works [CAI 00, WEI 02] have proposed numerical approaches to evaluate this quantity, whose the effect is to dissipate the HFWs and to avoid wave reflections at the interface between the discrete and continuum models.

In recent years, the bridging-scale methods have received much research interest, and several improvements, concerning the damping kernel and projection mechanism, have been proposed. In the first implementation of Wagner and Liu [WAG 03], the projection of the fine-scale solution onto the coarse-scale solution is apparently only performed at the interface using the approach of Adelman and Doll [ADE 76] (without introducing Lagrange multipliers). This approach has been improved by computing the interface nodes using Green's functions for lattices [PAR 05a, PAR 05b]. More recently, other enhancements have been proposed to join the coarse and fine scales in a BD, using the perfectly matched layer (PML) technique

[LI 06, TO 05]. As shown [XU 09], the performance of the BS methods based on PML is comparable to that of BD methods. However, the BD methods would be less costly, since they allow for reducing spurious wave reflections by only a correct setting of their parameters (no additional treatments are required).

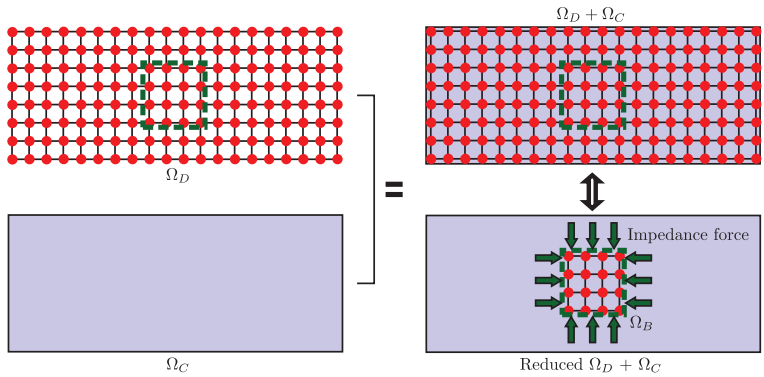

Figure 1.8. *Removal of unnecessary degrees of freedom in bridging-scale modeling*

1.3.4. *Other coupling techniques*

1.3.4.1. *Quasicontinuum method*

The quasicontinuum (QC) method was originally developed in the context of lattice statics at zero temperature (molecular mechanics) using empirical interatomic potentials [TAD 96b, TAD 96a]. Later on, it was extended to dynamic problems using the coarse grained energy and the Hamilton principle [LI 14, ROD 03, SHE 99]. The chief objective of the theory is to systematically coarsen a particle (atomistic) description by introducing kinematic constraints. These constraints are selected and designed so that the fully atomistic model is preserved in the regions of fine-scale effects and large number of particles (atoms) are collectively treated in the coarse-scale regions. The fully discrete model is then represented by a set of representative particles (mainly located in the fine-scale region), where the equation of motion has to be solved (Figure 1.9). The displacement of the non-representative particles is determined by kinematic constraints based on finite element meshing, of which the nodes are coincident with the representative particles (Figure 1.9).

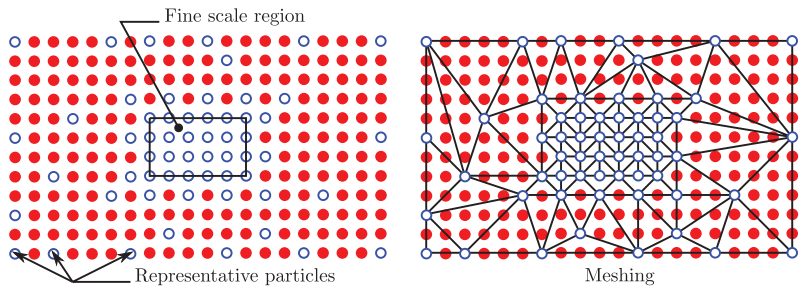

a) Selection of representative particles

b) Meshing for application of kinematic constraints

Figure 1.9. *Quasicontinuum model*

Although the imposed kinematic constraints significantly reduce the number of degrees of freedom (particles), the computational complexity of evaluating the generalized forces corresponding to the coarse-grained degrees of freedom (representative particles) still scales with the total number of particles in the system making computation on large systems intractable. Several approximations have been suggested in the literature to alleviate such difficulty [IYE 11, LI 14, ORT 01, ROD 03, SHE 99]. These include the mixed discrete (atomistic) and continuum formulations, or introduction of cluster summation rules on lattice sums. However, these approximations induce spurious forces, which can affect the solution accuracy. As shown in the literature [LI 14], the effects of these induced forces are more significant in the case of dynamic studies. These effects may even be more severe than the spurious reflections at the interface. Many strategies have been suggested to correct the errors incurred in these approximations [SHI 04, WEI 06], but they introduce undesirable seams in the process. Furthermore, recent numerical analysis suggests that the approximations introduced may not be consistent and stable, and can result in uncontrolled errors for rapid coarse-graining [DOB 08, DOB 10]. More recently, other works have proposed seamless QC formulations. However, they generally suffer from a lack of systematic convergence [IYE 11].

1.3.4.2. *Coupling of discrete and continuum meshless methods*

In this section, techniques used to couple discrete and continuum meshless methods are briefly reviewed. The readers are referred to [LIU 02] for more details. These techniques were first developed to couple smoothed particle hydrodynamics (SPH) and MD. In meshless methods, the studied domain is represented by a set of scattered particles (continuum particles) or nodes

without any connectivity between them. Each continuum particle has its corresponding smoothing length R, representing the influence domain, and length scale h, characterizing locally the domain discretization. The idea is that the continuum particles close to the discrete-continuum interface (transitional particles) also act as virtual discrete particles for the discrete model (Figure 1.10). To avoid interface problems, the length scale of the transitional particles must be graded down to the order of the discretization characteristic length of the discrete model. The communication between the coupled models can further be enhanced by using large transitional zone, in which the particles act both as continuum and discrete particles (Figure 1.10).

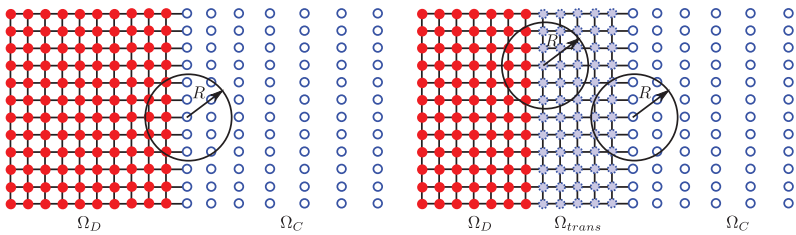

a) Coupling with reduced transitional zone b) Coupling with extended transitional zone

Figure 1.10. *Techniques for coupling discrete and continuum meshless methods*

1.4. Conclusion

Mainly, three coupling approaches can be used to couple discrete element method (DEM) with CMs: hierarchical, concurrent and hybrid hierarchical-concurrent approach. Among them, the concurrent approach is the most appropriate to study multi-scale problems in fast dynamics which is the scope of the present book. This chapter brought light to some important aspects related to this approach. First, the major difficulties that arise from application of this approach to couple DM and CM for dynamic studies were briefly outlined. These difficulties are mainly due to the different mechanical bases and analysis scales between the coupled methods. Then, the techniques most commonly used to overcome such difficulties were reviewed. Among these techniques, the BD technique seems best suited to develop a concurrent DEM-CM coupling approach for highly dynamic studies. Using this technique, spurious wave reflections can naturally be avoided without any additional filtering or damping. This can considerably reduce the computation time. The fine-scale solution is projected onto the coarse-scale solution in the bridging region at each time step. This projection mechanism naturally filters

the high-frequency portion of the fine-scale solution that is not supported by the admissible solution space of the coarse-scale model. This technique is then retained to develop the concurrent discrete-continuum coupling. The question that arises here is how to choose the CM that will be coupled with DEM. Chapter 2 tries to answer this question.